

Application of a novel 2D cadmium(II)-MOF in the formation of a photo-switch with substantial on-off ratio

Electronic Supporting Information

Materials

All chemicals used were purchased from Sigma-Aldrich and were of reagent grade. They were used without further purification.

Synthesis of [CdL(μ -1,3-SCN)₂]_n

A methanol solution of 3-ethoxysalicylaldehyde (1 mmol, 0.166 g) and N-ethyl-1,2-diaminoethane (1 mmol, 0.105 mL) was refluxed for 1 h to prepare a tetradentate N₂O₂ donor Schiff base 2-(2-(ethylamino)ethyliminomethyl)-6-ethoxyphenol (HL). The Schiff base was not isolated and was used directly for preparation of the complex. A methanol solution of cadmium(II) acetate dihydrate (1 mmol, 0.266 g) was added to the methanol solution of the Schiff base followed by addition of methanol solution of sodium thiocyanate (1mmol, 0.081 g) with constant stirring. The stirring was continued for an additional 20 min. Diffraction quality single crystals were obtained after few days on slow evaporation of the solution in open atmosphere.

Yield: 0.58 g (72%). Anal. Calc. for C₁₄H₁₉CdN₃O₂S (FW 405.80) : C, 41.44; H, 4.72; N, 10.35% Found: C, 41.36; H, 4.68; N, 10.42% IR (KBr, cm⁻¹): 1651 ($\nu_{C=N}$), 3228 (ν_{NH}), 2110, 2077 (ν_{SCN}); UV-Vis, λ_{max} (nm), [ϵ_{max} (L mol⁻¹ cm⁻¹)] (DMSO), 258 (1.06 × 10⁴), 336 (2.49 × 10³). ¹H NMR (DMSO-d₆) δ ppm: 8.1 (s, 1H); 6.7 (dd, 1H, J = 8,3Hz); 6.2 (t, 2H, J = 8 Hz); 3.5 (q, 2H); 3.9 (q, 2H); 2.6 (t, 2H); 2.7 (t, 2H); 1.2 (t, 3H); 1.1 (t, 3H).

Physical Measurements

Elemental analysis (carbon, hydrogen and nitrogen) was performed on a Perkin–Elmer 240C elemental analyzer. Infrared spectrum in KBr ($4500\text{--}500\text{ cm}^{-1}$) was recorded using a PerkinElmer FT-IR spectrum twospectrometer. Electronic spectrum in DMSO ($800\text{--}200\text{ nm}$) was recorded on a PerkinElmer Lambda 35 UV–Vis spectrophotometer. The ^1H NMR spectrum at 300 MHz was recorded in DMSO- d_6 on a Bruker DRX 300 Spectrometer. Fluorescence spectrum in DMSO was obtained in Shimadzu RF-5301PC spectrofluorometer at room temperature. Lifetime measurement was recorded using Hamamatsu MCP photomultiplier (R3809) and was analyzed by using IBHDAS6 software. The powder XRD data was collected on a Bruker D8 Advance X-ray diffractometer using Cu $K\alpha$ radiation ($\lambda = 1.548\text{ \AA}$) generated at 40 kV and 40 mA. The PXRD spectrum was recorded in a 2θ range of $5\text{--}50^\circ$ using 1-D Lynxeye detector at ambient conditions.

X-ray crystallography

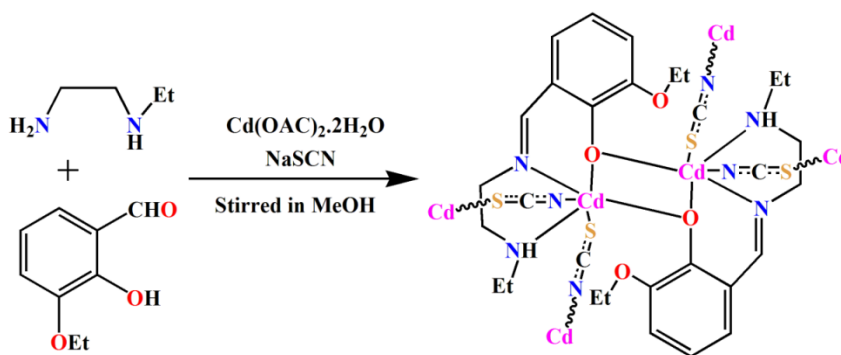
Single crystal of the complex having suitable dimensions, was used for data collection using a Bruker SMART APEX II diffractometer equipped with graphite-monochromated Mo $K\alpha$ radiation ($\lambda = 0.71073\text{ \AA}$) at 150 K. The molecular structure was solved using the SHELX-97 package.¹ Non-hydrogen atoms were refined with anisotropic thermal parameters. Hydrogen atoms were placed in their geometrically idealized positions and constrained to ride on their parent atoms. Multi-scan empirical absorption corrections were applied to the data using the program SADABS.²

Crystal data: formula = $\text{C}_{14}\text{H}_{19}\text{CdN}_3\text{O}_2\text{S}$, formula weight = 405.80, Temperature (K) = 150, crystal system = Orthorhombic, space group = *Pbca*, $a = 13.9096(3)\text{ \AA}$, $b = 10.5234(2)\text{ \AA}$, c

= 22.6923(5) Å, d_{calc} (gcm^{-3}) = 1.623, μ (mm^{-1}) = 1.447, $F(000)$ = 1632, total reflections = 44700, unique reflections = 2930, observed data [$I > 2\sigma(I)$] = 2585, $R(\text{int})$ = 0.040, R_1 , wR_2 (all data) = 0.0318, 0.0645, R_1 , wR_2 [$I > 2\sigma(I)$] = 0.0269, 0.0626.

Synthesis

The Schiff base ligand HL was prepared by the condensation of condensation of N-ethyl-1,2-diaminoethane with 3-ethoxysalicylaldehyde following the literature method.³⁻⁵ The ligand was not isolated and used directly for the preparation of the complex. The methanol solution of HL was made to react with methanol solution of cadmium(II) acetate dihydrate followed by the addition of sodium thiocyanate under stirring condition to produce the complex $[\text{CdL}(\mu\text{-}1,3\text{-SCN})_2]_n$. The potential tetradentate Schiff base, HL, here acts as a tridentate one and occupies three sites of the octahedral cadmium(II). The remaining sites are occupied by two thiocyanates and one phenoxo oxygen. Exploiting the end-to-end bridging capacity of thiocyanates, a two-dimensional coordination polymer, $[\text{CdL}(\mu\text{-}1,3\text{-SCN})_2]_n$ is formed. The formation of the complex is shown in Scheme S1.



Scheme S1. Synthetic route to the complex.

Hirshfeld Surface Analysis

Hirshfeld surfaces,⁶⁻⁸ and the associated two-dimensional (2D) fingerprint⁹⁻¹¹ plots were calculated using Crystal Explorer¹² with bond lengths to hydrogen atoms set to standard values¹³. For each point on the Hirshfeld isosurface, two distances, d_e (the distance from the point to the nearest nucleus external to the surface) and d_i (the distance to the nearest nucleus internal to the surface), are defined. The normalized contact distance (d_{norm}) based on d_e and d_i is given by

$$d_{\text{norm}} = \frac{(d_i - r_i^{\text{vdw}})}{r_i^{\text{vdw}}} + \frac{(d_e - r_e^{\text{vdw}})}{r_e^{\text{vdw}}}$$

where r_i^{vdw} and r_e^{vdw} are the van der Waals radii of the atoms. The value of d_{norm} is negative or positive depending on intermolecular contacts being shorter or longer than the van der Waals separations. The parameter d_{norm} displays a surface with a red–white–blue color scheme, where bright red spots highlight shorter contacts, white areas represent contacts around the van der Waals separation, and blue regions are devoid of close contacts. For a given crystal structure and set of spherical atomic electron densities, the Hirshfeld surface is unique¹⁴ and thus it suggests the possibility of gaining additional insight into the intermolecular interaction of molecular crystals.

Device fabrication

To get insight the electrical behavior we deposited thin film of our material on ITO coated glass substrate. First, for well dispersion, the synthesized material was mixed with DMSO in right proportion and was sonicated for 30 minutes. Then ITO coated glass substrates were cleaned with soap solution, acetone, ethanol, and distilled water sequentially by ultrasonication technique and dried in vacuum desiccator. To develop thin film on the cleaned ITO coated substrates, well dispersed solution was spun at 600 rpm for 2 minutes and thereafter, at 1200 rpm

for next 10 minutes, with the help of SCU 2700 spin coating unit. The as-deposited thin film was dried in a vacuum oven at temperature 100°C. The thickness of the developed thin film was measured as 800 nm. We deposited aluminum as front electrode on the top of the film through shadow mask by Vacuum Coating Unit 12A4D of HINDHIVAC under pressure 10^{-6} mbarr. The effective area of the film was maintained as 7.065×10^{-2} cm². For electrical characterization, the current-voltage characteristic was measured by two-probe technique with the help of Keithley 2400 source meter. All the preparation and measurements were performed under room temperature and in ambient condition.

Theoretical methods

The orthorhombic crystal structure was optimized with the density functional theory (DFT) method using the all-electron Dmol3 program code of Accelrys, Inc.¹⁵⁻¹⁷ [CdL(μ -1,3-SCN)₂]₈ complex with a cell formulae of C₁₁₂N₂₄O₁₆S₈Cd₈ was relaxed with the experimental unit cell parameters fixes ($a = 13.91 \text{ \AA}$ $b = 10.52 \text{ \AA}$ and $c = 22.69 \text{ \AA}$). The calculations were performed within the Generalized-Gradient Approximation (GGA) and the Perdew-Burke-Ernzerhof (PBE) formulation for the exchange-correlation functional^{18,19} using double numerical with polarization (DNP) basis set and a global orbital cutoff of 4.5 \AA^{-1} . The maximum number of numerical integration mesh points available in DMol3 was chosen for our computations, the threshold of density matrix convergence was set to 10^{-6} . The long-range dispersion correction has been included in the calculations with the Grimme's scheme.²⁰ Band structures were calculated along the k -vector of the first Brillouin zone of the crystal and Total and Partial density of states (TDOS and PDOS, respectively) were plotted with respect to the Fermi level, for comparison purposes.

Hydrogen bonding interactions

The hydrogen atom, H(2), attached to the nitrogen atom, N(2), is participated in hydrogen bonding interaction (Table S3) with the symmetry-related oxygen atom, O(2)^a {symmetry transformation ^a = 1-x,-y,1-z}, (Figure S3).

IR, electronic and fluorescence spectra

In the IR spectrum (Figure S4) of the complex, band corresponding to the azomethine (C=N) stretching vibration appears at 1651 cm⁻¹.^{4,21} The μ -1,3-mode of thiocyanate groups is confirmed by the splitting of absorption band corresponding to SCN-stretching vibration appearing at 2100 and 2076 cm⁻¹ (indicating S- and N- coordination modes respectively).²² In addition, two medium bands are observed at 848 and 744 cm⁻¹ related to ν (CS).²²⁻²⁵ The bands in the range of 2971-2862 cm⁻¹ are assigned due to alkyl C-H bond stretching vibrations.²⁶ IR spectrum of the complex exhibits a moderately strong, sharp peak at 3228 cm⁻¹, which is ascribed to the N-H stretching vibration.²⁶

Electronic spectrum was recorded in DMSO solution in the range 200–800 nm. The complex shows intense absorption bands at 258 and 336 nm which may be assigned as π - π^* and n - π^* transitions, respectively. The complex exhibits luminescence in DMSO medium at 419 nm on exciting at 348 nm, which may be assigned to the intra-ligand (π - π^*) fluorescence. The excitation and emission spectrum of complex is shown in Figure S5. The lifetime of the excited state is 12.63 ns at room temperature. Decay profile (Figure S6) was fitted to a multi-exponential model:

$$I(t) = \sum_i \alpha_i \exp(-t/\tau_i)$$

where, mono-exponential functions are used to fit the emission of the complex with and obtaining χ^2 close to 1, ($\chi^2 = 1.054994$).

Relative fluorescence quantum yield for the complex was measured in DMSO using quinine sulfate (in 0.5 (M) H_2SO_4 , $\phi = 0.54$) as the quantum yield standard.²⁷ The fluorescence quantum yield of the complex is 0.03552.

Powder X-ray diffraction

The experimental powder XRD patterns of the bulk product of the complex is in good agreement with the simulated XRD patterns from single crystal X-ray diffraction, confirming purity of the bulk sample. The simulated patterns was calculated from the single crystal structural data (cif file) using the CCDC Mercury software. Figure S7 show the experimental and simulated powder XRD patterns of the complex.

Hirshfeld surfaces

The Hirshfeld surfaces of the complex, mapped over d_{norm} , shape index and curvedness, is illustrated in Figure S8. The surfaces are shown as transparent to allow visualization of the molecular moiety around which they are calculated. The dominant interaction between $\text{C}\cdots\text{S}/\text{O}\cdots\text{H}$ atoms can be seen in the Hirshfeld surfaces as red spots on the d_{norm} surface in Figure S8. Other visible spots in the Hirshfeld surfaces correspond to $\text{H}\cdots\text{H}$ contacts. The small extent of area and light color on the surface indicate weaker and longer contact other than hydrogen bonds. The intermolecular interactions appear as distinct spikes in the 2D fingerprint plot (Figure S9). Complementary regions are visible in the fingerprint plots where one molecule acts as a donor ($d_e < d_i$) and the other as an acceptor ($d_e > d_i$). The fingerprint plots can be decomposed to highlight particular atom pair close contacts.²⁸ This decomposition enables

separation of contributions from different interaction types, which overlap in the full fingerprint. The proportion of C...S/S...C and O...H/H...O interaction comprises 4.9 and 5.3% of the Hirshfeld surfaces for each molecule. These interactions also appear as two distinct spikes in the 2D fingerprint plot (Figure S9). The upper spike corresponding to the donor spike represents the C...S interactions ($d_i = 0.73$, $d_e = 0.12$ Å) and the lower spike being an acceptor spike represents the S...C interactions ($d_e = 0.93$, $d_i = 0.74$ Å) in the Fingerprint plot as shown in Figure S9 (a).

References

- 1 G. M. Sheldrick, *Acta Cryst.*, 2008, **A64**, 112-122.
- 2 G. M. Sheldrick, *SADABS: Software for Empirical Absorption Correction*; Institut für Anorganische Chemie der Universität, University of Göttingen: Göttingen, Germany, 1999-2003.
- 3 A. Bhattacharyya, P. K. Bhaumik, P. P. Jana and S. Chattopadhyay, *Polyhedron*, 2014, **78**, 40-45.
- 4 M. Das, K. Harms and S. Chattopadhyay, *Dalton Trans.*, 2014, **43**, 5643-5647.
- 5 A. Bhattacharyya, K. Harms and S. Chattopadhyay, *Inorg. Chem. Commun.*, 2014, **48**, 12-17.
- 6 M. A. Spackman and D. Jayatilaka, *CrystEngComm*, 2009, **11**, 19-32.
- 7 F. L. Hirshfeld, *Theor. Chim. Acta*, 1977, **44**, 129-138.
- 8 H. F. Clausen, M. S. Chevallier, M. A. Spackman and B. B. Iversen, *New J. Chem.*, 2010, **34**, 193-199.
- 9 A. L. Rohl, M. Moret, W. Kaminsky, K. Claborn, J. J. McKinnon and B. Kahr, *Cryst. Growth Des.*, 2008, **8**, 4517-4525.
- 10 A. Parkin, G. Barr, W. Dong, C. J. Gilmore, D. Jayatilaka, J. J. McKinnon, M. A. Spackman and C. C. Wilson, *CrystEngComm*, 2007, **9**, 648-652.
- 11 M. A. Spackman and J. J. McKinnon, *CrystEngComm*, 2002, **4**, 378-392.
- 12 S. K. Wolff, D. J. Grimwood, J. J. McKinnon, D. Jayatilaka and M. A. Spackman, *Crystal Explorer 2.0*; University of Western Australia: Perth, Australia, 2007.
<http://hirshfeldsurfacenet.blogspot.com/>.

13 F. H. Allen, O. Kennard, D. G. Watson, L. Brammer, A. G. Orpen and R. J. Taylor, *J. Chem. Soc., Perkin Trans.*, 2 1987, S1-S19.

14 J. J. Kinnon, M. A. Spackman and A. S. Mitchell, *Acta Crystallogr.*, 2004, **B60**, 627-668.

15 B. Delley, *J. Chem. Phys.*, 2000, **113**, 7756-7764.

16 B. Delley, *J. Phys. Chem.*, 1996, **100**, 6107-6110.

17 B. Delley, *J. Chem. Phys.*, 1990, **92**, 508-517.

18 J. P. Perdew, K. Burke and M. Ernzerhof, *Phys. Rev. Lett.* 1996, **77**, 3865-3868.

19 J. P. Perdew, J. A. Chevary, S. H. Vosko, K. A. Jackson, M. R. Pederson, D. J. Singh and C. Fiolhais, *Phys. Rev. B. Condens. Matter*, 1992, **46**, 6671-6687.

20 S. Grimme, *J. Comput. Chem.*, 2006, **27**, 1787-1799.

21 M. Das, S. Chatterjee, K. Harms, T. K. Mondal, and S. Chattopadhyay, *Dalton Trans.*, 2014, **43**, 2936-2947.

22 Chemistry of pseudohalides, A. Golub (Ed), Elsevier, 1986.

23 A. Sabtini and I. Bertini, *Inorg chem.*, 1965, **4** 959-961.

24 M. A. S. Goher, L. A. Al-shatti, and F. A. Mautner, *Polyhedron*, **16**, 889-895.

25 R. J. H. Clark, and C. S. Williams, *Spectrochim. Acta*, 1966, **22**, 1081-1090.

26 S. Roy, K. Harms, and S. Chattopadhyay, *Polyhedron*, 2015, **91**, 10-17.

27 M. Das, B. N. Ghosh, A. Valkonen, K. Rissanen, and S. Chattopadhyay, *Polyhedron*, 2013, **60**, 68-77.

Table S1: Selected bond lengths (Å) of the complex.

Cd(1)–O(1)	2.271(2)	Cd(1)–N(3)	2.294(3)
Cd(1)–N(1)	2.249(3)	Cd(1)–O(1) ^a	2.374(2)
Cd(1)–N(2)	2.366(3)	Cd(1)–S(1) ^b	2.7543(12)

Symmetry transformations ^a = 1-x, -y, 1-z; ^b = 3/2-x, 1/2+y, z.**Table S2:** Selected bond angles (°) of the complex.

O(1)–Cd(1)–N(1)	92.77(10)
O(1)–Cd(1)–N(2)	150.54(9)
O(1)–Cd(1)–N(3)	77.84(9)
O(1)–Cd(1)–O(1) ^a	82.48(7)
S(1) ^b –Cd(1)–O(1)	97.62(6)
N(1)–Cd(1)–N(2)	114.61(12)
N(1)–Cd(1)–N(3)	169.60(12)
O(1) ^a –Cd(1)–N(1)	92.14(9)
S(1) ^b –Cd(1)–N(1)	82.24(8)
N(2)–Cd(1)–N(3)	75.50(11)
O(1) ^a –Cd(1)–N(2)	85.69(9)
S(1) ^b –Cd(1)–N(2)	85.69(9)
O(1) ^a –Cd(1)–N(3)	91.04(9)
S(1) ^b –Cd(1)–N(3)	94.47(7)
S(1) ^b –Cd(1)–O(1) ^a	174.39(5)

Symmetry transformations ^a = 1-x, -y, 1-z; ^b = 3/2-x, 1/2+y, z

Table S3: Hydrogen bond distance (Å) and angle (°) of the complex.

D–H···A	D–H	H···A	D···A	∠D–H···A
N(2)–H(2)···O(2) ^a	0.78	2.30	3.067(4)	172(4)

D, donor; H, hydrogen; A, acceptor. Symmetry transformation ^a = 1-x, -y, 1-z.

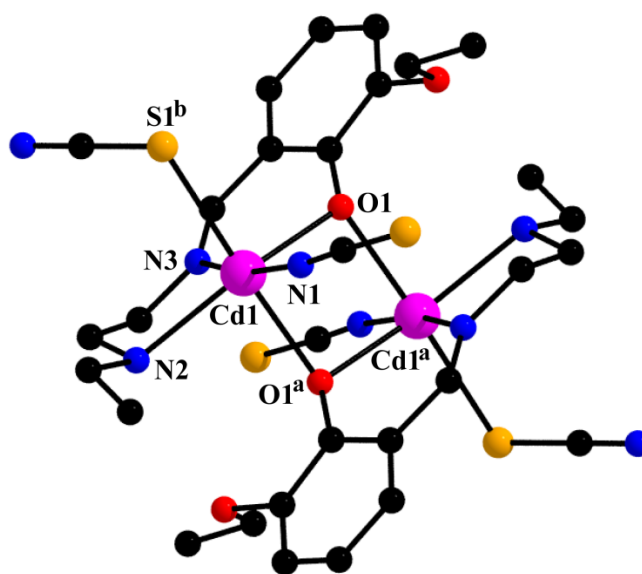


Figure S1: Perspective view of the complex with selective atom-numbering scheme. Hydrogen atoms are not shown for clarity. Symmetry transformations ^a = 1-x, -y, 1-z; ^b = 3/2-x, 1/2+y, z.

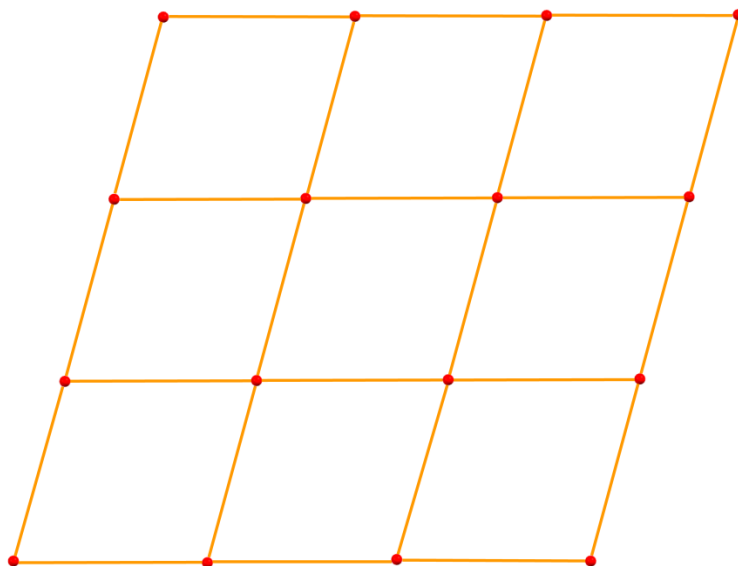


Figure S2: A perspective view of (4,4) Square grid topology of complex.

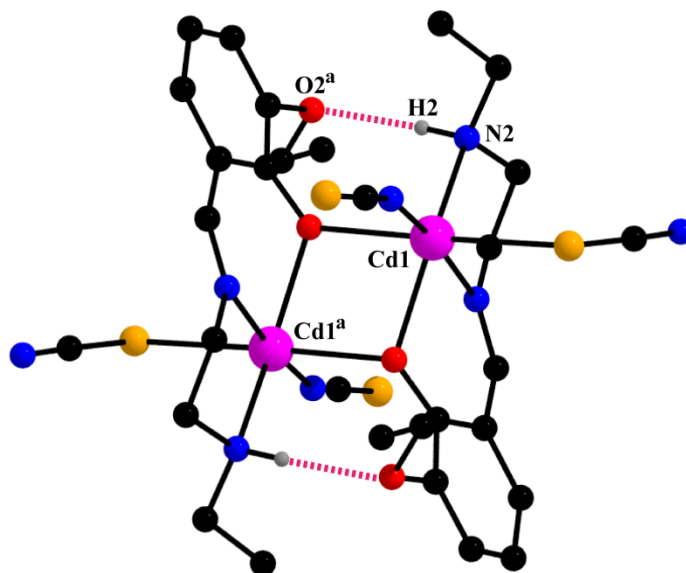


Figure S3: H-bonded dimer of the complex. Selected hydrogen atoms are omitted for clarity. Symmetry transformation, ^a = 1-x, -y, 1-z.

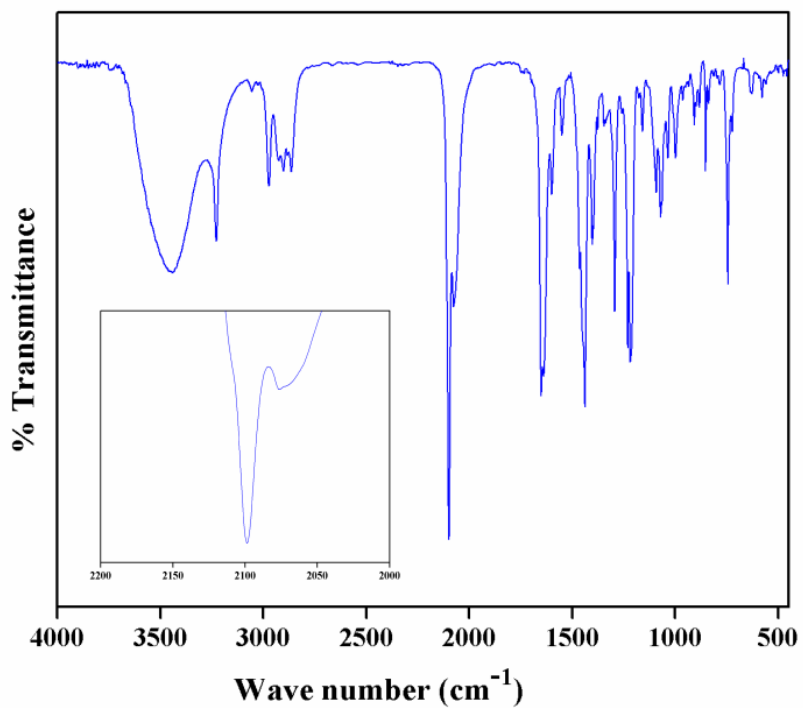


Figure S4: IR spectrum of the complex.

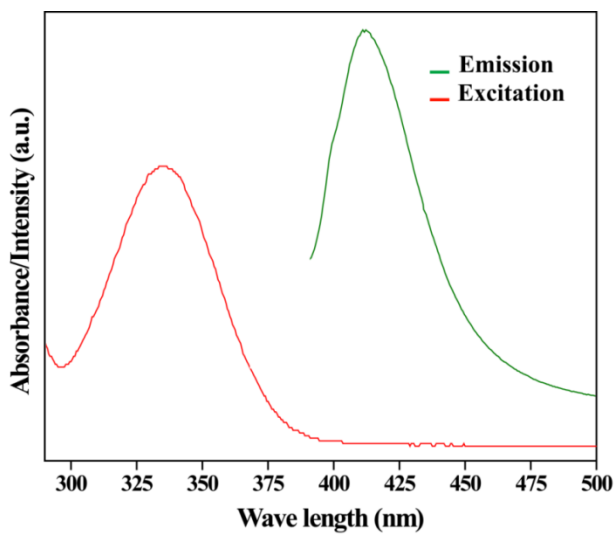


Figure S5: Excitation and emission spectrum of the complex in DMSO solution.

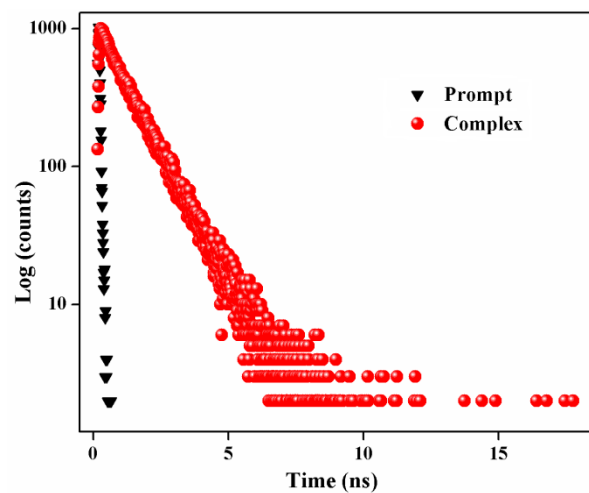


Figure S6: Lifetime decay profile of the complex.

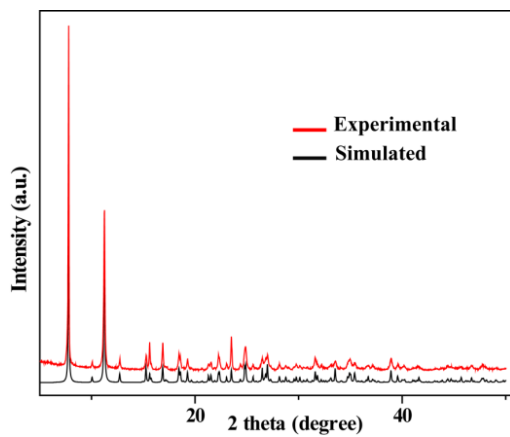


Figure S7: Experimental and simulated powder XRD patterns of the complex confirming the purity of the bulk materials.

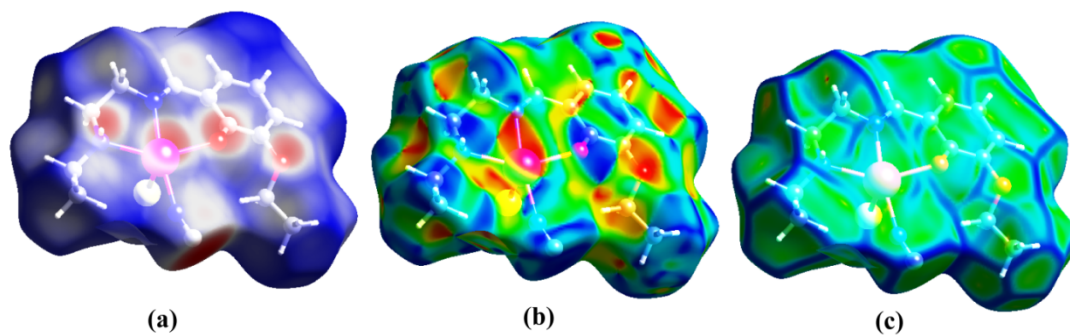


Figure S8: Hirshfeld surfaces mapped with (a) d_{norm} , (b) shape index (c) curvedness for complex.

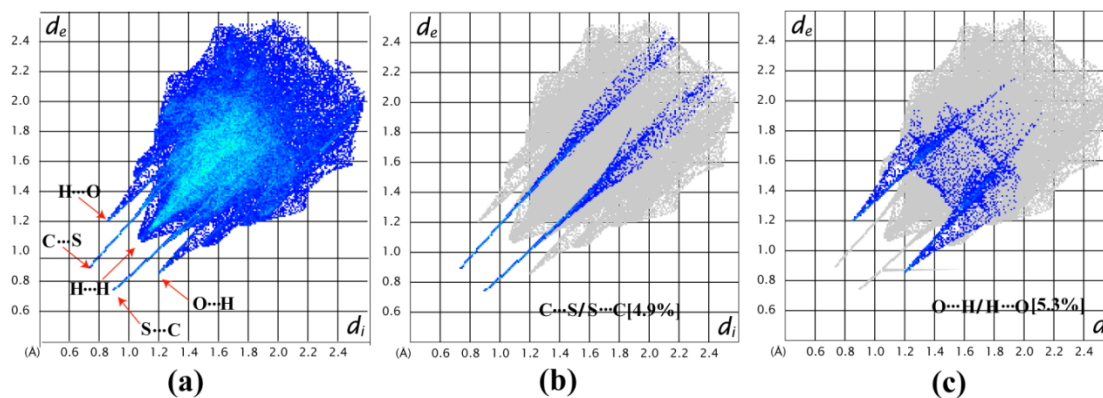


Figure S9: (a) 2D fingerprint plots; (b) 2D fingerprint plots with C \cdots S/S \cdots C interactions (c) 2D fingerprint plots with O \cdots H/H \cdots O interactions highlighted in color.